HHS Public Access

Author manuscript

Nature. Author manuscript; available in PMC 2019 July 01.

Published in final edited form as:

Nature. 2011 February 03; 470(7332): 110–114. doi:10.1038/nature09766.

Timing of plant immune responses by a central circadian regulator

Wei Wang[1,*], **Jinyoung Yang Barnaby**[1,*,†], **Yasuomi Tada**[1,†], **Hairi Li**[2], **Mahmut Tör**[3], **Daniela Caldelari**[1,†], **Dae-un Lee**[1], **Xiang-Dong Fu**[2], and **Xinnian Dong**[1]

[1]Department of Biology, P. O. Box 90338, Duke University, Durham, North Carolina 27708, USA.

[2]Department of Cellular and Molecular Medicine, University of California, San Diego, La Jolla, California 92093, USA.

[3]National Pollen and Aerobiology Research Unit (NPARU), University of Worcester, Henwick Grove, Worcester WR2 6AJ, UK.

Abstract

The principal immune mechanism against biotrophic pathogens in plants is the resistance (R)-gene-mediated defence1. It was proposed to share components with the broad-spectrum basal defence machinery2. However, the underlying molecular mechanism is largely unknown. Here we report the identification of novel genes involved in *R*-gene-mediated resistance against downy mildew in *Arabidopsis* and their regulatory control by the circadian regulator, CIRCADIAN CLOCK-ASSOCIATED 1 (CCA1). Numerical clustering based on phenotypes of these gene mutants revealed that programmed cell death (PCD) is the major contributor to resistance. Mutants compromised in the *R*-gene-mediated PCD were also defective in basal resistance, establishing an interconnection between these two distinct defence mechanisms. Surprisingly, we found that these new defence genes are under circadian control by CCA1, allowing plants to 'anticipate' infection at dawn when the pathogen normally disperses the spores and time immune responses according to the perception of different pathogenic signals upon infection. Temporal control of the defence genes by CCA1 differentiates their involvement in basal and *R*-gene-mediated defence. Our study has revealed a key functional link between the circadian clock and plant immunity.

The life cycles of biotrophic pathogens of plants are intimately linked with host metabolism controlled by the cycle of day and night. Hence, their interactions with the host may be

Correspondence and requests for materials should be addressed to X.D. (xdong@duke.edu).

†Present addresses: Crop Systems and Global Change Laboratory, United States Department of Agriculture, Agricultural Research Service, Plant Sciences Institute, Room 342, Building 001, BARC-West, 10300 Baltimore Avenue, Beltsville, Maryland 20705,USA(J.Y.B.); Life Science Research Centre, Institute of Research Promotion, Kagawa University, 2393 Ikenobe, Miki-cho, Kita-gun, Kagawa 761-0795, Japan (Y.T.); Plant Molecular Biology, University of Lausanne, CH-1015 Lausanne, Switzerland (D.C.).

*These authors contributed equally to this work.

Author Contributions J.Y.B., W.W., Y.T., D.C. and D.-u.L. identified new components in *R*-gene-mediated resistance; J.Y.B., W.W. and Y.T. showed that RPP4 controls two major defence responses by phenotypic clustering analysis; J.Y.B., W.W. and M.T. demonstrated that *R*-gene-mediated resistance shares common components with basal defence machinery; W.W., J.Y.B., H.L., X.-D.F. and X.D. verified the circadian regulator CCA1 plays a key role in timing the different immune responses; W.W., J.Y.B. and X.D. wrote the manuscript with inputs from all co-authors. All authors discussed the results and commented on the manuscript.

The authors declare no competing financial interests.

Supplementary Information is linked to the online version of the paper at www.nature.com/nature.

dictated by the circadian clock. This is especially likely as plants do not have specialized immune cells and their immune responses have to be finely balanced with other cellular functions. However, a link between the circadian clock and plant defence has never been firmly established[3].

The major plant defence strategy against biotrophic pathogens is resistance (*R*)-gene-mediated immunity. Detection of a pathogen-encoded virulence effector by the R protein triggers programmed cell death (PCD) and several other physiological responses collectively known as the hypersensitive response[4]. The effector-specific *R*-gene-mediated resistance may share components with the broad-spectrum basal defence machinery[2]. But how these components are differentially regulated is still unclear.

We chose to study resistance against *Hyaloperonospora arabidopsidis* (*Hpa*) because this obligate biotrophic oomycete pathogen causes downy mildew disease on *Arabidopsis* leaves through clearly defined infection steps[5], allowing better dissection of the corresponding resistance mechanisms blocking these steps. The *Arabidopsis* Columbia (Col-0) accession is resistant to the *Hpa* Emwa1 isolate due to the presence of the *R* gene, *RPP4* (ref. 6). We performed a time-course expression profiling of wild type and *rpp4* (Supplementary Fig. 1) in response to *Hpa* Emwa1 infection. Based on the phenotype development and defence marker gene expression (Supplementary Fig. 2a, b), we identified 106 genes differentially expressed in wild type and *rpp4* at 2 days post inoculation (dpi) (Supplementary Fig. 2c). These candidate genes were induced earlier than the previously reported immune regulators including *EDS5, PAD4, PBS3, ICS1, NDR1* and *EDS1* (ref. 7), which were known to function downstream of *R* gene activation.

We inoculated the T-DNA insertion mutants (from the ABRC and NASC Stock Centres) of these 106 candidate genes with *Hpa* Emwa1 and identified 22 mutants that displayed enhanced susceptibility compared to wild type based on sporangiophore growth and other disease symptoms (for example, chlorosis) by microscopic inspection. For most of the 22 genes, at least two homozygous mutant T-DNA alleles were tested (Supplementary Fig. 3 and Supplementary Tables 1 and 2).

To identify specific resistance defects in the mutants, we stained the infected plants with lactophenol trypan blue (LTB) 7 dpi and scored for the occurrence of the seven phenotypes represented in Supplementary Fig. 4a. As shown in Supplementary Fig. 4b, the *rpp4* mutant had the highest percentage of leaves with sporangiophores (SPP), confirming that its resistance to *Hpa* Emwa1 is completely compromised as SPP indicates completion of the infection cycle. Wild type had the highest score of discrete hypersensitive response (DIH), which was defined by the small cluster of infected host cells that underwent PCD, a phenotype associated with *R*-gene-mediated resistance. The phenotype scores are also presented numerically in Fig. 1a and the mutants are ranked on the basis of their SPP scores.

Hierarchical clustering of the mutants using their phenotype scores (Fig. 1a) put these 22 gene mutants into two groups (Fig. 1b). Similar groupings are also obtained with data from three biological replicates (Supplementary Fig. 5). Eigenvectors derived from principal component analysis indicate that 63.8% of the phenotype variations could be accounted for

by PC1 with indicators of resistance, DIH and expanding hypersensitive response (EXH), as positive contributors and disease phenotypes, SPP and free hypha (FRH), as negative contributors (Fig. 1c). If PC2 was also considered, six out of the seven phenotypes had significant contributions.

The Group 1 mutants (red numbers in Fig. 1b and Supplementary Fig. 5) seem to be defective in *R*-gene-mediated PCD (low DIH and EXH scores) with high disease symptoms (FRH and SPP). In contrast, the Group 2 mutants (blue numbers) appeared to be intact in PCD with high EXH and DIH scores and milder symptoms (low FRH and SPP scores). To determine the resistance defects in Group 2 mutants, we examined them for other *R*-gene-mediated physiological responses, such as accumulation of phenolic compounds involved in cell wall strengthening against pathogen penetration and deposition of callose after *Hpa* Emwa1 inoculation. We found that Mutant 16 (tyrosine aminotransferase 3) was defective in phenolic compound accumulation at the site of pathogen penetration (Supplementary Fig. 6a) and Mutants 12 (lipase class 3 family protein) and 14 (cyclic nucleotide gated channel 3) showed a deficiency in callose deposition in response to *Hpa* Emwa1 similar to that observed in *rpp4* (Supplementary Fig. 6b).

Collectively, these observations suggest that RPP4 regulates at least two separate responses (Fig. 1d): Group 1 genes are required for R-mediated PCD, as mutations in these genes led to low DIH and EXH scores and formation of FRH, TRN, and SPP. The Group 2 genes are probably involved in defence responses other than PCD, such as callose deposition and phenolic compound accumulation. Loss of these latter functions resulted in pathogen penetration even in the presence of PCD. One important conclusion from these data is that PCD is the predominant resistance response against *Hpa* Emwa1 because the Group 1 mutants were more susceptible, on the basis of the SPP scores (except Mutant 12), than the Group 2 mutants (Fig. 1a, b). This is supported by the eigenvector composition where PC1 (DIH and EXH) was the major contributor to the phenotypic variations (Fig. 1c). This finding is consistent with the fact that *Hpa* Emwa1 is an obligate biotrophic pathogen. Suicidal death of the host cell means the end of the pathogen life cycle. The functional diversity of the Group 1 genes indicates that RPP4-mediated PCD is orchestrated by changes in multiple biological processes, rather than a single triggering event.

We also subjected the 22 defence gene mutants to infection by the virulent isolate, *Hpa* Noco2, to which a cognate *R* gene is absent in Col-0. We found that 10 of the mutants displayed significantly enhanced disease susceptibility (Fig. 2a) demonstrating that these defence genes are involved in both *R* gene-specific PCD and general basal resistance. To determine whether the observed defect in *Hpa* Emwa1 resistance is RPP4-specific or due to compromised basal defence, we infected the mutants with *Hpa* isolates, Cala2 and Hiks1, which are known to have cognate *R* genes, *RPP2* and *RPP7,* respectively, in the Col-0 background[7,8]. None of the mutants showed compromised resistance (Fig. 2b and Supplementary Table 1) indicating that the deficiency in resistance against *Hpa* Emwa1 is *RPP4* gene-specific. However, a few of the mutants did show defects in RPS2-mediated resistance to a bacterial pathogen *Pseudomonas syringae* pv. *maculicola* ES4326 carrying AvrRpt2 *(Psm* ES 4326/AvrRpt2) (Supplementary Fig. 7a). Three of them were also

hypersusceptible to *Psm* ES4326 in the absence of the AvrRpt2 signal (Supplementary Fig. 7b).

We next subjected all of the 22 mutants to microbial-associated molecular pattern (MAMP) treatments including EF-Tu (elf18) and flagellin (flg22) to examine the interconnection between *R*-gene-mediated resistance and MAMP-triggered basal immunity. We found that Mutant 1, mutated in the leucine-rich repeat receptor-like kinase (LRR-RLK; AT1G35710), was insensitive to elf18 (Fig. 2c, d). Because Mutant 1 also showed the highest level of susceptibility to *Hpa* Emwa1 (Fig. 1a), we propose that this LRR-RLK is a link between MAMP-signalling and RPP4-mediated PCD and resistance. Although MAMP-triggered immunity is not typically associated with PCD, MAMP signalling components have been implicated previously in PCD. Mutation of the *Arabidopsis* BRI1-associated receptor kinase 1 (BAK1), which is a MAMP-coreceptor required for responses to elf18 and flg22 (ref. 9), was shown to cause spreading necrosis upon pathogen challenge, indicating that BAK1 is an inhibitor of PCD[10]. However, silencing BAK1 in *Nicotiana benthamiana* blocked the cell death induced by the oomycete elicitor INF1 (ref. 11), consistent with our finding that a MAMP signalling component is involved in PCD resistance against oomycete infection.

Our genetic data showed that R-mediated resistance and basal defence share common components. This raises the question of how activation of similar sets of genes causes PCD in RPP4-specific resistance against *Hpa* Emwa1 and non-specific basal resistance against *Hpa* Noco2. To understand the differential regulation of these immune mechanisms, we analysed the promoter regions of these 22 genes. Using the Athena program (http://www.bioinformatics2.wsu.edu/Athena/), we found significant enrichment of the ‘evening element’, which is regulated both positively and negatively by the circadian regulator, CCA1 (refs 12, 13). Further examination showed that 14 of the 22 genes contain either evening element and/or the CCA1-binding site and/or have rhythmic expression patterns (Fig. 3a)[14]. Interestingly, the promoter region of *RPP4* also contains two evening elements and its expression shows a circadian rhythm.

To confirm the involvement of the circadian clock in defence, we first examined the responses of clock mutants to *Hpa* Emwa1. The infection was carried out at dawn, the time when *Hpa* spores are normally disseminated in nature[15]. The *cca1* mutant (Salk_067780) and *ztl-4* (a mutant of *ZEITLUPE*)[16] showed compromised resistance whereas a CCA1-overexpression line ($CCA1_{OE}$)[17] showed enhanced resistance (Fig. 3b). Surprisingly, *lhy,* the mutant of the *CCA1* homologue, *LATE AND ELONGATED HYPOCOTYL* (*LHY*)[18] responded as wild type.

We next examined the expression patterns of all 22 defence genes in wild type, *rpp4* and *cca1* every 2 h in a 46-h time-course, with and without infection by *Hpa* Emwa1. Because of the large number of samples involved, we used the innovative high throughout RNA annealing selection ligation-sequencing (RASL-seq) technology[19] for expression analysis (Supplementary Table 3 and Methods).

As shown in Fig. 3c, consistent with the genetic data, the rhythmic expression of *LHY* was not significantly perturbed by infection in either wild type or *rpp4*. This indicates that RPP4-

mediated defence does not disrupt the overall running of the clock, but rather engages CCA1. This specific sensitivity of *CCA1* to infection conditions was confirmed using a transgenic line expressing *CCA1:LUC* (ref. 16, Supplementary Fig. 8a). To eliminate the effects of light changes on *CCA1* expression, we also performed infection in transgenic plants carrying the *CCA1:LUC* and *LHY:LUC* reporters[16] under the free-running light cycles (Supplementary Fig. 8b). Similar to the RASL-seq results, *LHY:LUC* expression remained unchanged, whereas *CCA1:LUC* expression was significantly induced and became arrhythmic upon *Hpa* Emwa1 challenge.

Conveniently, the stable expression pattern of *LHY* served as an internal control for the quality of RNA preparations and RASL-seq. Based on the non-negative matrix factorization (NMF) algorithm[20], the 22 RPP4-regulated genes fit best into two clusters (Fig. 3a and Supplementary Figs 9 and 10). The membership distance of each gene to its cluster is illustrated by the circle radius in Supplementary Fig. 11a. These two clusters corresponded roughly to the two phenotypic groups determined through genetic analysis (Figs 1 and 3a). Most of the Cluster 1 genes containing evening element in their promoters are involved in *R*-gene-mediated PCD and were therefore the focus of further concern (Fig. 3c). The expression patterns of the Cluster 2 genes are shown in Supplementary Fig. 11b.

Consistent with the fact that evening element is enriched in the Cluster 1 gene promoters (Fig. 3a), the weighted mean expression of these genes largely overlaps with the expression patterns of *CCA1* (Fig. 3c). In wild-type control (Col CK), Cluster 1 genes showed a rhythmic expression pattern with a single sharp peak every evening. In *cca1* (*cca1* CK), the expression peaks were greatly diminished, confirming that CCA1 is an activator of these defence genes.

The rhythmic expression of the defence genes in the absence of pathogen indicates that plants are programmed to ‘anticipate’ infection according to a circadian schedule. The CCA1-mediated pulse expression of the defence genes coincides with the time of *Hpa* sporulation which mainly occurs at night and the time of spore dissemination which takes place at dawn[15]. To test this, we performed *Hpa* Emwa1 infection not only at the normal ‘dawn’ infection time but also at ‘dusk’. We found that if the plants were inoculated at dusk, when infection was unexpected, significantly higher levels of susceptibility were observed in both wild type and *rpp4* (Fig. 3d). CCA1 clearly has a role in conferring resistance at dawn because in *cca1,* more *Hpa* Emwa1 growth was observed compared to wild type. However, no further increase in susceptibility was observed in *cca1* if inoculation was carried at dusk because *CCA1* and the CCA1-regulated defence genes are not expressed at this time.

In response to *Hpa* Emwa1 infection, Cluster 1 genes showed drastically different expression patterns in wild type (Col EMWA1) and *rpp4* (*rpp4* EMWA1) (Fig. 3c). Without *RPP4,* the expression of the defence genes peaked at the 6-, 16- and 24-h time points which coincided with the expected time of *Hpa* spore germination, formation of penetration hyphae and establishment of primary haustoria in mesophyll cells, respectively[5]. This pattern of expression may explain how these defence genes contribute to the basal resistance against *Hpa* infection. Consistent with CCA1 having a role in basal resistance, $CCA1_{oe}$ was more resistant to *Hpa* Noco2 than wild type (Supplementary Fig. 12). However, understanding the

signalling events between the pathogen and CCA1 leading to this specific timing of defence gene expression will require future research.

In the presence of RPP4, the 6-h expression peak was diminished (Col EMWA1, Fig. 3c). The subsequent perception of the pathogen effector by RPP4 led to the gradual and sustained expression of defence genes. We propose that the prolonged expression of these defence genes, which are normally pulse-expressed at dawn, results in PCD of the infected host cells and pathogen resistance. Consistent with it being a key positive regulator of Cluster 1 defence genes involved in RPP4-mediated PCD, knocking out CCA1 function significantly lowered the average DIH score (a measure of host cell death) in *cca1* after *Hpa* Emwa1 infection (Fig. 3e).

How RPP4 interacts with CCA1 to control the defence gene expression requires further investigation. The spatial resolution of the expression data from the *Hpa* Emwa1-infected samples, homogenized from both infected and uninfected cells, was not enough to allow detailed dissection of the contribution of RPP4, CCA1 and unknown pathogenic signals. Nevertheless, RPP4 clearly is not only a target gene of CCA1, but also a partner of CCA1 in regulating the defence genes as their patterns of expression were disturbed in *rpp4* (Fig. 3c and Supplementary Fig. 2c).

Establishment of a molecular link between the plant circadian clock and R-mediated defence reveals a new interface between the plant host and biotrophic pathogens. Although the interactions between *R* genes and the circadian clock have yet to be studied genetically and at the molecular level, this study indicates a central role of the circadian clock in balancing growth and defence. As summarized in Fig. 3f, we hypothesize that the Cluster 1 genes are pulse-expressed to minimize adverse effects to the host in anticipation of infection under normal conditions and during basal defence. In contrast, detection of a pathogenic effector by the R protein may disrupt this control, leading to PCD of the infected cell and R-mediated resistance, which is a much stronger and signal-specific immune response. There is also an increasing body of evidence indicating that animal immune response is influenced by the circadian clock[21]. Understanding the molecular link between the circadian clock and immunity therefore has broad implications in biology.

METHODS SUMMARY

Hyaloperonospora arabidopsidis (Hpa) propagation and inoculation were performed as described[6,22]. Ten-day-old plants were inoculated with the asexual spores suspension (5×10^5 spores per ml) of *Hpa.* Unless specified, the *Hpa* infection was always performed at dawn of the growth chamber's photoperiod. *Hpa* Emwa1-inoculated samples were collected at 0, 0.5, 2 and 4 days post inoculation (dpi). ATH1 GeneChip (Affymetrix) was used for microarray. The arrays were normalized and analysed as described previously[23]. Disease phenotypes were scored after trypan blue staining at 7 dpi[24]. Significance of the phenotypic scores was determined based on binomial distribution. Disease phenotypic analysis was performed using hierarchical clustering with distance measured by the standard correlation (average linkage; scale 0–1). The significance of the clustering (bootstrap 100,000 times) was measured by the approximately unbiased *P*-values (0–100%, the higher the number the

more significant[25]). Callose deposition was detected after aniline blue staining[26]. Accumulation of phenolic compounds was examined under ultraviolet illumination (Leica). Root length and fresh weight assays for elf18 sensitivity were performed as described previously[9]. The evening element enrichment was determined based on hypergeometric distribution. Samples for RASL-seq were prepared according to ref. 19. Non-negative matrix factorization algorithm was used to cluster the genes[20]. RNA extraction was performed as described previously[27]. cDNA synthesis (Superscript III, Invitrogen) and quantitative PCR (SYBR Green, Qiagen) were performed according to the manufacturer's protocols. For *Pseudomonas* infection, 4-week-old plants were inoculated with 10 mM $MgCl_2$ or *Pseudomonas syringae maculicola* ES4326 with or without the effector *AvrRpt2* (OD_{600}=0.001). The *in planta* bacterial growth was measured at 3 dpi. For diurnal luciferase measurement, protein was extracted and bioluminescence intensity was measured using the Luciferase Assay System (Promega) according to manufacturer's protocol. Ten-day-old plate-grown plants were used for free-running test (details in Methods).

Full Methods and any associated references are available in the online version of the paper at www.nature.com/nature.

METHODS

Arabidopsis and *Hyaloperonospora arabidopsidis* (Hpa) growth conditions

Arabidopsis seedlings were grown for 10 days at 16–18 °C, 12-h day length, 80–100% relative humidity before *Hpa* infection through spray of a spore suspension (5×10^5 spores per ml in distilled H_2O) at dawn according to the photoperiod of the plant growth chamber. *Hpa* Emwa1 and *Hpa* Noco2 were subcultured and inocula prepared using methods modified from previous reports[6,22].

RNA extraction and quantitative PCR analysis

RNA extraction was performed as described previously[27]. cDNA synthesis (Superscript III, Invitrogen) and quantitative PCR (SYBR Green PCR kit, Qiagen) were performed according to the manufacturer's protocols.

Microarray

Ten-day-old wild-type and *rpp4* seedlings were inoculated with *Hpa* Emwa1 and samples were collected at 0, 0.5, 2 and 4 days after inoculation. Total RNA was isolated from the frozen material using the Qiagen RNeasy kit. RNA probes were labelled using the GeneChip Eukaryotic Small Sample Target Labelling Assay Version II and hybridized on the Affymetrix ATH1 GeneChip (Santa Clara). Two biological replicates were performed. The data presented in this publication have been deposited in NCBI's Gene Expression Omnibus and are accessible through GEO Series accession number GSE22274 (http://www.ncbi.nlm.nih.gov/geo/query/acc.cgi?acc=GSE22274).

Normalization and mixed-model analysis

The mixed-model software used to normalize globally all arrays and to identify differentially expressed probe sets was as described previously[23]. Expression indices were used to

calculate *P*- and *q*-values for pairwise comparisons of all probe sets across all treatments. R^2 values for the CEL files are as follows (Col_0d: 1 vs 2(0.98); Col_0.5d: 1 vs 2(0.97); Col_2d: 1 vs 2(0.98); Col_4d: 1 vs 2(0.96); rpp4_0d, 1 vs 2 (0.98); rpp4_0.5d, 1 vs 2 (0.97); rpp4_2d, 1 vs 2 (0.98); rpp4_4d, 1 vs 2 (0.97)).

Phenotyping mutants in response to *Hpa* infection

Seven days after inoculation with *Hpa* Emwa1 infection, phenotypes were scored following lactophenol trypan blue staining[24]. Leaves were vacuum-infiltrated twice in a solution of phenol, lactic acid, glycerol and water (1:1:1:1) plus 2.5 mg ml^{-1} trypan blue. The tubes containing the samples were placed in a boiling water bath for 2 min and allowed to cool for overnight. The leaves were destained in the chloral hydrate solution and then treated with 70% glycerol. Whole leaves were analysed and photographed with a MZ8 stereo microscope (Leica) and a PM-C35 camera (Olympus). Detailed examination of *Hpa* structures was conducted with an Olympus BX60F compound microscope and differential interference contrast (DIC) optics. Leaves were stained for callose as described with modifications[26]. To visualize callose, leaves were cleared in a solution of ethanol and acetic acid (3:1), stained with 0.02% aniline blue in 100 mM sodium phosphate buffer (pH 9) for 1h, and examined with an Axio imager wide field fluorescence microscope (Zeiss). To detect phenolic compounds, leaves were examined under ultraviolet fluorescent illumination (Leica DMRB). To measure *Hpa* Noco2 infection, infected leaves were collected in 1 ml water, and sporangiospores were counted.

elf18 and flg22 treatment

Wild-type *Arabidopsis* (Col-0), *efr* and candidate mutant plants were grown on MS11% sucrose medium (pH 5.7) plate with 1 μM elf18 or MS alone as a control under continuous light for 9 days for root length assay[9]. For fresh weight assay, plants were grown on MS11% sucrose medium (pH 5.7) plate for 4 days (16/8 light/dark cycle), transferred into water containing 50 nM elf18 or water as a control, and fresh weight was measured 6 days after elf18 treatment. flg22 (10 nM) was infiltrated into 3-week-old plants for the induction of callose deposition.

Promoter element analysis

The statistical significance of over-represented transcription factor (TF) binding elements was calculated using a hypergeometric probability model. The following equation was used to provide the *P*-values:

$$P = 1 - \sum_{x=0}^{k-1} \frac{\binom{m}{x}\binom{N-m}{n-x}}{\binom{N}{n}}$$

N is the total number of promoters in the genome, *n* is the number of promoters in the genome containing the specified TF-binding element, *m* is the size of the selected set of promoters, and *x* is the number of promoters with the specified element in the selected set.

Because multiple hypotheses were tested in the analysis, the Bonferroni correction was used. The genome-wide occurrences of these elements in the promoters are used as controls.

RASL-seq

The growth conditions (12/12 light/dark cycle, 16–18 °C, 80–100% humidity), which were optimized for *Hpa* infection, were different from those used in traditional circadian studies[12,13]. Samples were collected every 2 h after inoculation and the remaining plants were kept to ensure successful pathogen inoculation. Total RNA for each sample (1 μg) was used for RASL-seq. Primer (gene-specific with flanking 5′ or 3′ universal sequences) annealing to mRNA and ligation were carried out according to ref. 19. Bar-coded primers were then added to each sample to convert the ligated products to individual libraries, which were pooled from all samples and subjected to multiplex sequencing using Solexa GAII (Illumina).

RASL-seq data analysis

The readings from RASL-seq were assumed Poisson distribution. Only those samples with mean readings significantly above zero (Pr (mean=0)<0.01) were considered for further analysis. The reading for each sample was first divided by the corresponding reading of control, ubiquitin 5 (*UBQ5;* AT3G62250), and then standardized. The resulting matrix was used for clustering analysis.

Non-negative matrix factorization (NMF) algorithm[20] was used to cluster the genes. The number of the clusters was determined by comparing the cophenetic correlation coefficient for a range of cluster numbers (from 2 to 22). The cophenetic correlation coefficient is a measurement of how faithfully the result of NMF clustering preserves the pairwise distances between the original data points. As shown in Supplementary Fig. 9, two clusters generated the highest cophenetic correlation coefficient, which means two clusters can reflect the original data more faithfully than more clusters. Divergence was used as the update rule and cost measurement. Minimum of the data was subtracted from the data matrix to ensure that there were no negative numbers in the matrix. Because the NMF algorithm iteratively updates the decomposition of the data matrix, 300 runs with 10,000 iterations/run were performed to reach the convergence (Supplementary Fig. 10). The membership indicators from NMF clustering were used as weights to calculate the weighted mean expression pattern shown in Fig. 3c. The weights were also used to determine the radii of circles in Supplementary Fig. 11a. Smaller radius indicates a higher membership of the gene to the corresponding cluster.

Bioluminescence detection

Protein was extracted and bioluminescence intensity measured using the Luciferase Assay System (Promega) according to the manufacturer's manual. A Victor3 (PerkinElmer) multilabel reader was used to detect the bioluminescence. Substrate (100 μl) was added using an automatic injector. After 3 s shaking, 2 s delay, the signal was captured for 20 s. Log_{10} transformation was performed to the raw signals to ensure the normal distribution of the data. After subtraction of the blank, the data were normalized according to the total

protein concentrations determined by the Bradford method (Bio-Rad). The resulting data were then standardized.

Free-running test

Seeds were sterilized in 2% Plant Preservative Mixture (PPM, Plant Cell Technology) in the dark at 4 °C for 4 days before plating on MS plate (3% sucrose, 1.5% agar) and grown in a 12/12 h light/dark growth chamber for 9 days. At the dawn and the dusk of the ninth day, 2.5 mM luciferin in 0.05% Triton-X 100 was sprayed onto the seedlings. At the dawn of the tenth day, the seedlings were treated by distilled H_2O or *Hpa* Emwa1 before being placed in a constant light chemiluminescence box. The bioluminescence signals were captured by CCD.

Supplementary Material

Refer to Web version on PubMed Central for supplementary material.

Acknowledgements

We thank S. Brady for performing mixed model ANOVA of the data and advice on data analyses; J. Li for sharing the protocol for elf18 treatment, E. Tobin for providing the $CCA1_{OE}$ transgenic line, R. McClung for *CCA1:LUC, LHY:LuC, ztl-4* lines. H. Lu for helpful discussion of the work, F. Ausubel, P. Benfey, S. Brady, J. Siedow and R. Mohan for critiquing the manuscript This work was supported by a grant from NSF (MCB-0519898) to X.D. and a grant (HG004659) to X.-D.F.

References

1. Jones JD & Dangl JL The plant immune system. Nature 444, 323–329(2006). [PubMed: 17108957]
2. Tao Y et al. Quantitative nature of *Arabidopsis* responses during compatible and incompatible interactions with the bacterial pathogen *Pseudomonas syringae*. Plant Cell 15, 317–330 (2003). [PubMed: 12566575]
3. Roden LC & Ingle RA Lights, rhythms, infection: the role of light and the circadian clock in determining the outcome of plant-pathogen interactions. Plant Cell 21, 2546–2552 (2009). [PubMed: 19789275]
4. Lam E, Kato N & Lawton M Programmed cell death, mitochondria and the plant hypersensitive response. Nature 411, 848–853 (2001). [PubMed: 11459068]
5. Donofrio NM & Delaney TP Abnormal callose response phenotype and hypersusceptibility to *Peronospoara parasitica* in defence-compromised *Arabidopsis* nim1–1 and salicylate hydroxylase-expressing plants. Mol. Plant Microbe Interact 14, 439–450 (2001). [PubMed: 11310731]
6. Holub EB, Beynon JL & Crute IR Phenotypic and genotypic characterization of interactions between isolates of *Peronospora parasitica* and accessions of *Arabidopsis thaliana*. Mol. Plant Microbe Interact 7, 223–239 (1994).
7. van der Biezen EA, Freddie CT, Kahn K, Parker JE & Jones JD *Arabidopsis RPP4* is a member of the *RPP5* multigene family of TIR-NB-LRR genes and confers downy mildew resistance through multiple signalling components. Plant J. 29, 439–451 (2002). [PubMed: 11846877]
8. McDowell JM et al. Downy mildew (Peronospora parasitica) resistance genes in Arabidopsis vary in functional requirements for NDR1, EDS1, NPR1 and salicylic acid accumulation. Plant J. 22, 523–529 (2000). [PubMed: 10886772]
9. Chinchilla D et al. Aflagellin-induced complex of the receptor FLS2 and BAK1 initiates plant defence. Nature 448, 497–500 (2007). [PubMed: 17625569]
10. Kemmerling B et al. The BRI1-associated kinase 1, BAK1, has a brassinolide-independent role in plant cell-death control. Curr. Biol 17, 1116–1122 (2007). [PubMed: 17583510]

11. Heese A et al. The receptor-like kinase SERK3/BAK1 is a central regulator of innate immunity in plants. Proc. Natl Acad. Sci. USA 104, 12217–12222 (2007). [PubMed: 17626179]
12. Harmer SL et al. Orchestrated transcription of key pathways in *Arabidopsis* by the circadian clock. Science 290, 2110–2113 (2000). [PubMed: 11118138]
13. Harmer SL & Kay SA Positive and negative factors confer phase-specific circadian regulation of transcription in *Arabidopsis*. Plant Cell 17, 1926–1940 (2005). [PubMed: 15923346]
14. Michael TP et al. Network discovery pipeline elucidates conserved time-of-day-specific cis-regulatory modules. PLoS Genet 4, e14 (2008). [PubMed: 18248097]
15. Slusarenko A & Schlaich NL Downy Mildew of Arabidopsis thaliana caused by Hyaloperonospora parasitica (formerly Peronospora parasitica). Mol. Plant Pathol 4, 159–170 (2003). [PubMed: 20569375]
16. Salome PA & McClung CR *PSEUDO-RESPONSE REGULATOR 7* and *9* are partially redundant genes essential for the temperature responsiveness of the *Arabidopsis* circadian clock. Plant Cell 17, 791–803 (2005). [PubMed: 15705949]
17. Wang ZY & Tobin EM Constitutive expression of the CIRCADIAN CLOCK ASSOCIATED 1 (CCA1) gene disrupts circadian rhythms and suppresses its own expression. Cell 93, 1207–1217 (1998). [PubMed: 9657153]
18. Schaffer R et al. The late elongated hypocotyl mutation of *Arabidopsis* disrupts circadian rhythms and the photoperiodic control of flowering. Cell 93, 1219–1229 (1998). [PubMed: 9657154]
19. Yeakley JM et al. Profiling alternative splicing on fiber-optic arrays. Nature Biotechnol. 20, 353–358 (2002). [PubMed: 11923840]
20. Tamayo P et al. Metagene projection for cross-platform, cross-species characterization of global transcriptional states. Proc. Natl Acad. Sci. USA 104, 5959–5964 (2007). [PubMed: 17389406]
21. Bryant PA, Trinder J& Curtis, N. Sick and tired: does sleep have a vital role in the immune system? Nature Rev. Immunol 4, 457–467 (2004). [PubMed: 15173834]
22. Tor M et al. *Arabidopsis* SGT1b is required for defense signaling conferred by several downy mildew resistance genes. Plant Cell 14, 993–1003 (2002). [PubMed: 12034892]
23. Brady SM et al. A high-resolution root spatiotemporal map reveals dominant expression patterns. Science 318, 801–806 (2007). [PubMed: 17975066]
24. Bowling SA, Clarke JD, Liu Y, Klessig DF & Dong X The *cpr5* mutant of *Arabidopsis* expresses both NPR1-dependentand NPR1-independent resistance. Plant Cell 9, 1573–1584(1997). [PubMed: 9338960]
25. Suzuki R &Shimodaira, H. Pvclust: an R package for assessing the uncertainty in hierarchical clustering. Bioinformatics 22, 1540–1542 (2006). [PubMed: 16595560]
26. Adam L & Somerville SC Genetic characterization of five powdery mildew resistance loci in *Arabidopsis thaliana*. Plant J. 9, 341–356 (1996). [PubMed: 8919911]
27. Cao H, Bowling SA, Gordon S & Dong X Characterization of an *Arabidopsis* mutant that is nonresponsive to inducers of systemic acquired resistance. Plant Cell 6, 1583–1592 (1994). [PubMed: 12244227]

a

No.	Description	SPP	TRN	OOS	FRH	FHI	EXH	DIH
RPP4	RPP4	98*	55*	73*	100*	25*	8*	3*
1	LRR-kinase	78*	10*	88*	88*	93*	20*	5*
2	Calcineurin-like phosphoesterase	78*	15*	100*	100*	100*	65	13*
3	ADR1-like1	75*	0	80*	95*	85*	5*	3*
4	Aspartic protease 38	68*	13*	95*	90*	95*	18*	3*
5	UDP-glucosyl transferase 72E1	65*	18*	95*	90*	93*	18*	8*
6	Ankyrin	65*	13*	93*	95*	83*	28*	10*
7	Disease resistance protein	65*	15*	90*	80*	90*	45*	43*
8	Protein kinase family protein	65*	0	95*	73*	95*	15*	25*
9	ABC transporter family protein	58*	0	93*	93*	95*	8*	0*
10	ATPase-like domain containing protein	55*	10*	60*	88*	95*	18*	8*
11	Ankyrin repeat protein	55*	3*	85*	90*	45	43*	28*
12	Lipid class 3 family protein	55*	23*	100*	55*	100*	58	13*
13	Constitutive shade avoidance 1	43*	50*	75*	50*	75*	25*	25*
14	Cyclic nucleotide gated channel 3	40*	10*	83*	13	93*	85*	55
15	Lipid transfer family protein	38*	0	88*	43*	88*	60	8*
16	Tyrosine aminotransferase 3	28*	5*	95*	35*	93*	60	28*
17	Glycoside hydrolase	25*	5*	78*	35*	78*	40*	40*
18	Cold-responsive protein	25*	3*	95*	30*	85*	65	48
19	Aspartyl protease family protein	20*	5*	90*	38*	90*	70	50
20	BON-association protein 1	20*	8*	73*	30*	85*	78*	35*
21	LRR-kinase	8	0	60*	28*	58*	80*	50
22	Ser/Thr protein kinase family protein	8	0	68*	40*	73*	83*	38*
WT	Wild type	5	0	48	15	40	63	55

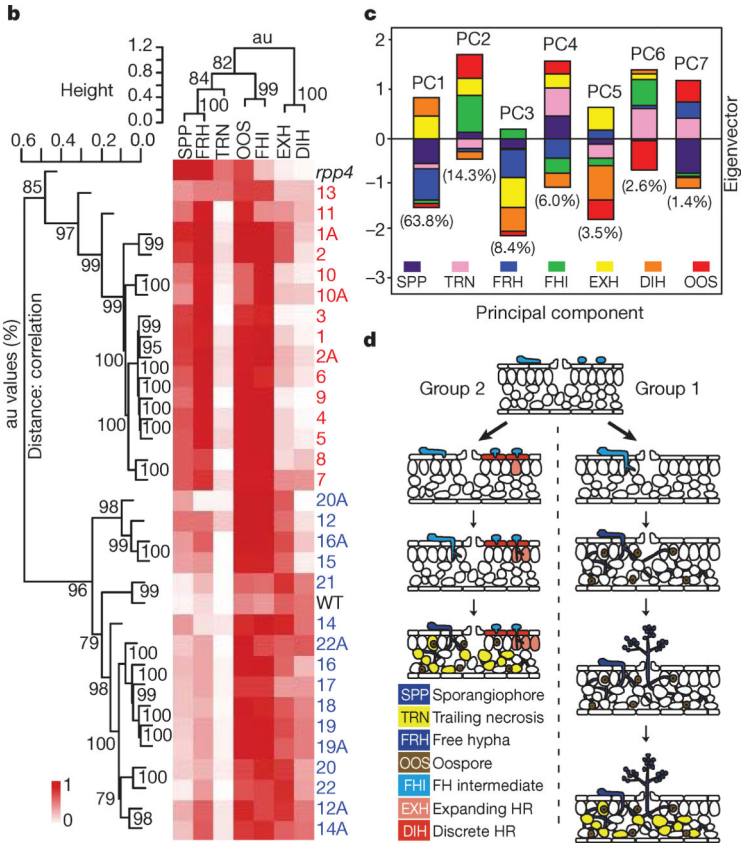

Figure 1 |. Phenotypic analyses discovered two distinct RPP4-mediated resistance responses against Hp*a* Emwa1.

a, Phenotype scores (percentage in 40 leaves per genotype). SPP, sporangiophore; TRN, trailing necrosis; OOS, oospore; FRH, free hypha; FHI, free hyphal intermediate; EXH, expanding hypersensitive response; DIH, discrete hypersensitive response. **P*<0.05. **b**, Mutants were clustered on the basis of their phenotype scores in Fig. 1a. Second allele, 'A'. Group 1, red; Group 2, blue. au, Approximately unbiased *P*-values (0–100%, the higher the number the more significant). **c**, Eigenvectors derived from PCA. The percentage of phenotypic variations captured by each PC is shown. **d**, A diagram showing that the Group 1 mutants are defective in RPP4-mediated PCD, whereas the Group 2 mutants are compromised in formation of physical/chemical barriers with intact PCD.

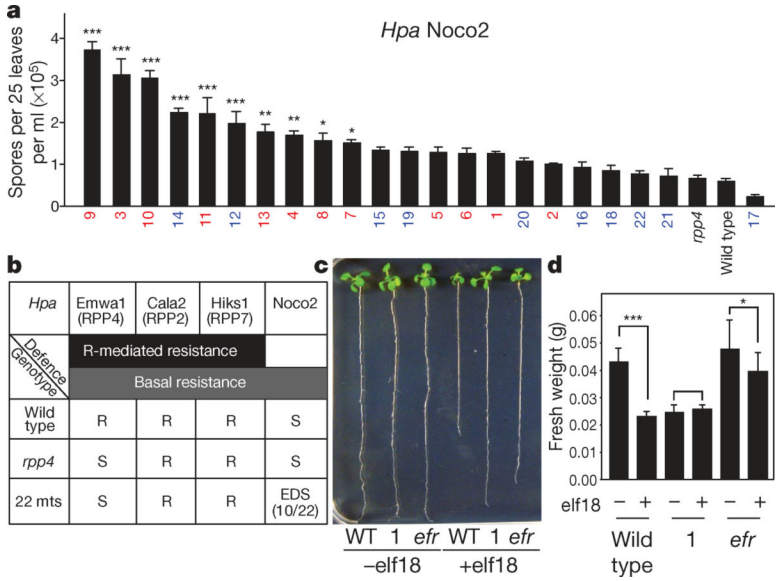

Figure 2 |. Some of the RPP4-mediated resistance mutants are also compromised in basal defence.

a, Enhanced disease susceptibility to *Hpa* Noco2 based on sporangiospore count 7 dpi (n=3). **b**, Summary of the infection tests on the 22 defence gene mutants (22 mts) using different *Hpa* isolates. S, susceptible; R, resistant; EDS, enhanced disease susceptibility. **c**, Root length measurements 9 days after elf18 treatment (n=3). *efr;* efl18 receptor mutant. **d**, Fresh weight measurements 6 days after elf18 treatment (n=3). *P<0.05, **P<0.01, ***P<0.001.

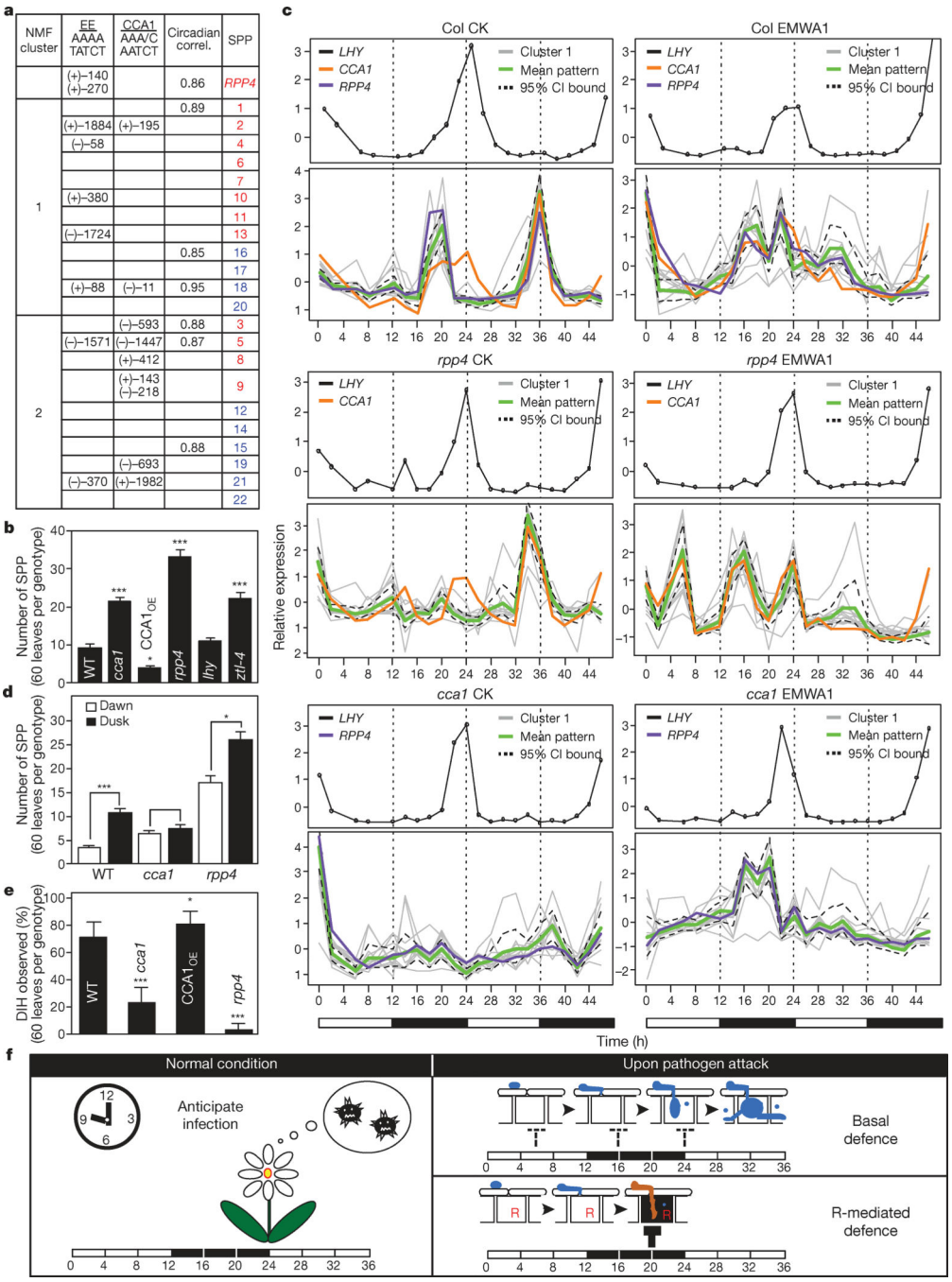

Figure 3 |. The circadian regulator, CCA1, controls the defence gene expression and the timing of immune responses.

a, Enrichment of evening element (EE) ($P<10^{-5}$). NMF, non-negative matrix factorization; CCA1, CCA1-binding sites; Circadian correl., circadian correlations[14]. +, sense; −, antisense. **b**, SPP count 7 dpiby *Hpa* Emwa1 ($n=3$). **c**, Time-course expression of NMF Cluster 1 genes. CI, confidence interval; CK, control; EMWA1, *Hpa* Emwa1 inoculated. White bars, day; black bars, night. **d**, SPP count after *Hpa* Emwa1 infection at dawn or dusk ($n=3$). **e**, Occurrence of DIH 7 dpi by *Hpa* Emwa. **f**, A model showing circadian regulation

of the defence genes in anticipation of infection under normal conditions, in basal and *R*-gene-mediated resistance. The blocked arrows represent defence against infection.